Title: Thermal filtering reveals a cryptic reservoir of thermotolerant yeasts in Sub-Antarctic soils

Luis A. Saona[1,2,3], Macarena Las Heras [4], José Benavides-Parra[1,5], Javiera I. Cajas[5], Fernanda Jeria-Osorio[5], Julian F. Quintero-Galvis[2,6], Jennifer Molinet[7],and Pablo Villarreal[5,8*]

[1] *Facultad de Química y Biología, Departamento de Biología, Universidad de Santiago de Chile, Santiago, 9170022, Chile.*

[2] *ANID-Millennium Nucleus of Patagonian Limit of Life (LiLi), Valdivia, Chile.*

[3] *Centro Científico y Tecnológico de Excelencia Ciencia & Vida, Fundación Ciencia & Vida, Huechuraba, Santiago, Chile.*

[4] *Facultad de Medicina, Centro de Genética y Genómica, Clínica Alemana Universidad del Desarrollo, Santiago, Chile.*

[5] *ANID-Millennium Science Initiative-Millennium Institute for Integrative Biology (iBio), Santiago, Chile.*

[6] *Departamento de Ciencias, Facultad de Artes Liberales, Universidad Adolfo Ibáñez, Santiago, Chile.*

[7] *Facultad de Ingeniería, Instituto de Ciencias Aplicadas, Centro de Investigación e Innovación, Universidad Autónoma de Chile, Santiago, Chile*

[8] *Centro de Genómica y Bioinformática, Facultad de Ciencias, Ingeniería y Tecnología, Universidad Mayor, Santiago, Chile.*

**Corresponding author.*

Email address: pablo.villarreal@umayor.cl

Graphical Abstract

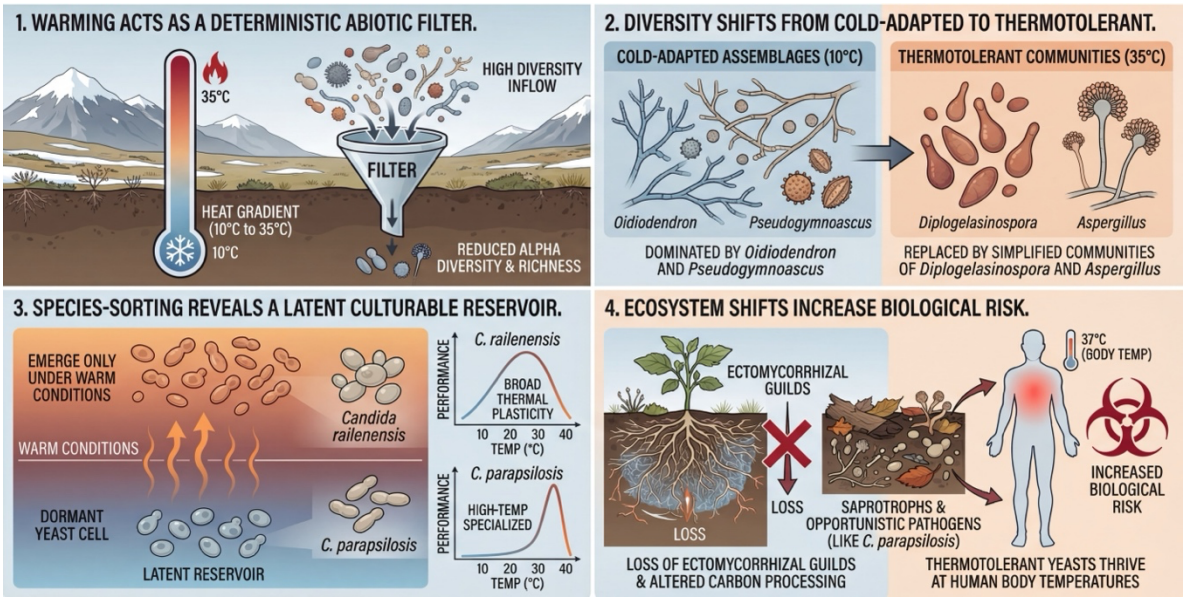

*Created with AI

Abstract

Global climate change is accelerating ecological transformation in Sub-Antarctic ecosystems, where resident biota exhibit narrow thermal tolerances. While microbial responses to warming are increasingly documented, the role of soil yeasts, key players in organic matter decomposition, remains poorly understood. Here, we show that warming acts as a deterministic filter, triggering a profound community restructuring that favors a cryptic reservoir of thermotolerant taxa. Using species-sorting and thermal profiling, we found that elevated temperatures (up to 35°C) significantly reduced alpha diversity and richness. This filtering shifted communities from cold-adapted assemblages to simpler, thermotolerant lineages. Thermal sorting revealed hidden culturable diversity, notably an increase in *Candida* spp., with *Candida railenensis* and *Candida parapsilosis* found only under warm conditions. Physiological profiling showed *C. railenensis* had broad thermal plasticity, while *C. parapsilosis* was high-temperature specialized. Additionally, warming nearly eliminated ectomycorrhizal guilds and increased saprotrophs, suggesting shifts in carbon processing and organic matter decomposition. Furthermore, our results indicate that sustained warming reduces functional redundancy and broadens reservoirs for opportunistic pathogens such as *C. parapsilosis*, which thrive near human body temperatures. These findings highlight the importance of including yeasts in climate models to predict future biogeochemical changes and biological risks in warming cold ecosystems.

Keywords: Global climate change, yeasts, Sub-Antarctic, microcosms, diversity, thermotolerance

Introduction

Global climate change is accelerating ecological transformation at an unprecedented rate across biomes. One of the primary anthropogenic stressors is the ongoing rise in temperature, which directly alters ecosystem dynamics and indirectly influences water availability, nutrient flows, and biodiversity patterns (Pendlebury & Barnes-Keoghan, 2007, Berdugo *et al.*, 2018, Delgado-Baquerizo *et al.*, 2018, Intergovernmental Panel on Climate, 2023). While these effects are increasingly well-documented in temperate forests and the polar cryosphere (Meir, Cox & Grace, 2006), high-latitude and Sub-Antarctic ecosystems remain comparatively understudied. These regions are especially vulnerable due to their historical climatic stability and the narrow thermal tolerance of their resident biota (Saona *et al.*, 2025, Zhang *et al.*, 2025). Recent studies in South America indicate that temperatures will increase and aridification will progress, posing significant risks to soil structure, vegetation productivity, and biogeochemical cycles (Barnes-Keoghan & Pendlebury, 2023). In this context, understanding how microbial communities, especially assemblages and their metabolic functions, respond to such shifts is essential for predicting broader ecosystem trajectories under global warming scenarios (Delgado-Baquerizo *et al.*, 2016, Delgado-Baquerizo *et al.*, 2018, Abs, Chase & Allison, 2023).

Microorganisms play a central role in terrestrial ecosystems, driving decomposition, nutrient cycling, and plant-soil feedback (Jansson & Hofmockel, 2020). Their diversity, rapid life cycles, and metabolic plasticity make them highly responsive to environmental fluctuations, including those induced by temperature shifts (Knight *et al.*, 2024). However, the relationship between microbial community structure and ecosystem function is not necessarily linear (Allison & Martiny, 2008). Recent evidence shows that microbial composition, functional traits, and evolutionary processes can interact to modulate ecosystem-level outcomes in complex ways (Yurkov & Pozo, 2017, Rodriguez Amor & Dal Bello, 2019, Diaz-Colunga *et al.*, 2022).

Warming can act as a selective pressure, altering community assembly trajectories and shifting ecosystem states toward lower functional redundancy or reduced resilience by favoring thermotolerant lineages over cold-adapted specialists (Yurkov & Pozo, 2017, Yurkov, 2018, Smith *et al.*, 2022). Moreover, microbial communities may exhibit eco-evolutionary feedback, in which shifts in community structure influence adaptive dynamics, a phenomenon particularly relevant under continuous climatic pressures. (Yurkov, 2018, Runnel *et al.*, 2025).

Microbial restructuring is not merely a taxonomic shift, it poses profound risks to ecosystem stability and biosecurity (Cavicchioli *et al.*, 2019). The replacement of specialized, cold-adapted taxa by thermotolerant lineages can disrupt delicate plant-soil feedbacks and alter nutrient-cycling rates, potentially destabilizing carbon storage in these vulnerable biomes (Delgado-Baquerizo *et al.*, 2016, Delgado-Baquerizo *et al.*, 2018). Furthermore, the deterministic selection of latent, heat-tolerant microorganisms, including taxa with opportunistic pathogenic potential, raises significant concerns about the emergence of fungal diseases in a warming world (Casadevall, Kontoyiannis Dimitrios & Robert, 2019). Understanding these community-level reorganizations is therefore vital for assessing the resilience of Sub-Antarctic forests and their capacity to maintain essential ecological services under future climate scenarios.

Within this context, the species sorting framework provides a robust conceptual basis for understanding community reassembly along environmental gradients. This process often relies on selecting taxa from a microbial seed bank, a reservoir of dormant or low-abundance organisms that can rapidly resuscitate when environmental conditions favor their specific traits (Litchman & Thomas, 2022). The success of these organisms is governed by their Thermal Performance Curves (TPCs), which define the physiological limits and optimal growth temperatures of each taxon (Alster, Weller & von Fischer, 2018, Ramond, Galand & Logares, 2025). While these dynamics have been studied in other microbes, the role of yeasts as a "cryptic reservoir" of diverse thermal traits remains largely unexplored (Burman & Bengtsson-Palme, 2021, Wieczynski *et al.*, 2021, Smith *et al.*, 2022). Furthermore, the deterministic selection of these latent microorganisms raises significant concerns: warming may favor the emergence of opportunistic pathogens, whose TPCs allow them to thrive as thermal thresholds are exceeded.

To understand this pattern, we studied yeast communities in rhizosphere soils from a Sub-Antarctic environment along a thermal gradient. We tested the hypothesis that warming constrains stochastic assembly, shifting the balance toward a deterministic regime in which the thermal niches of constituent taxa, defined by their TPCs, strictly predict community composition. Using a dual approach of ITS2 metabarcoding and culture-dependent thermal profiling, we linked taxonomic shifts directly to physiological limits. We show that yeast diversity and composition are significantly altered by temperature. These changes are consistent with the species-sorting paradigm: warming acts as an abiotic filter, favouring yeasts with high thermal tolerance

and reshaping communities through deterministic rather than stochastic processes. Our results expand understanding of microbial assembly under climate stress and highlight the importance of including yeasts in global change frameworks. Microorganisms and specialized yeasts also inform discussions of microbial functional similarity and redundancy, especially in ecosystems where warming exceeds microbial tolerance.

Materials and Methods

Sample collection

Rhizosphere samples were obtained from the Karukinka Natural Park in the Sub-Antarctic region (53°42'S 69°18'O). Five squares of 10 x 10 meters were established (**Figure S1**). Each of these squares was at least 1 km apart. In each square, five soil samples (50 g each) were randomly collected from the top 10 cm of soil and combined in a sterile plastic bag. All samples were stored in 50 mL tubes and maintained at -80 °C until the analysis.

Species-sorting analysis

For each sampling, three independent replicates of 5 g were generated. Each replicate was incubated at one of four temperatures (10, 20, 30, and 35 °C) for eight weeks (**Figure S1**). This thermal gradient was selected to represent conditions ranging from current Sub-Antarctic soil temperatures to extreme thermal stress scenarios, aiming to trigger and capture the latent functional diversity reservoir that may respond to abrupt warming events. During incubation, soil microcosms were periodically rehydrated with sterile deionized water to maintain moisture levels (Smith *et al.*, 2022). Immediately after the 8-week incubation, 1 g of soil from each replicate was stored at −20 °C for subsequent DNA extraction and metabarcoding analyses. The remaining soil (~4 g) from each replicate was processed for culture-based isolation as follows: samples were washed with phosphate-buffered saline (PBS), and the suspension was plated onto YPD agar (1% yeast extract, 2% peptone, 2% glucose, 2% agar) supplemented with 100 µg/mL chloramphenicol. Plates were incubated at both 20 °C and the corresponding sorting temperature (10, 20, 30, or 35 °C). Once colonies developed, the five most abundant morphologically distinct colony types per plate were selected. As a control, yeasts were also directly isolated from untreated soil samples and incubated at 20 °C. Isolates were preserved at −80 °C in 20% glycerol until subsequent molecular identification.

DNA extraction and sequencing

DNA was extracted from each rhizosphere sample using the Zymo Quick-DNA bacterial/fungal extraction kit according to the manufacturer´s instructions. The DNA obtained was quantified using the Invitrogen™ Qubit™ 4 Fluorometer, and samples containing more than 2 ng/μl of DNA were used to generate the ITS amplicon library. The extracted DNA was used as a template to amplify the internal nuclear ribosomal transcribed spacer 2 (ITS2 region), using forward ITS3 (5'-GCATCGATGAAGAACGCAGC-3') and reverse ITS4 (5'-TCCTCCGCTTATTGATATAT-3') primers (White *et al.*, 1990). The PCR conditions used for ITS amplification were as follows: denaturation at 95 °C for 3 min, followed by 25 cycles of 95 °C for 30 s (denaturation), 55 °C for 30 s (annealing), and 72 °C for 30 s (extension). A final annealing step was performed at 72 °C for 5 min. Libraries were prepared using the Illumina DNA Prep Kit according to the manufacturer's protocol. The libraries were then sequenced on the Illumina MiSeq using a Mid-Output Kit with 300-bp paired-end reads at the University of Chile sequencing facility. The total number of raw reads obtained is shown in **Table S1**.

Processing of ITS2 amplicon sequence data

Raw 300-bp paired-end reads from the MiSeq run were first demultiplexed and primers removed in QIIME 2 (v2022.8) (Bolyen *et al.*, 2019) using the Cutadapt plugin, yielding 45 sample-specific FASTQ pairs. Demultiplexed reads were then imported into R (v4.1.2) and processed with DADA2 (v1.20) (Callahan *et al.*, 2016). To ensure high-quality data, sequences were filtered, allowing a maximum of expected errors (maxEE = 2) for both forward and reverse reads. The first 1 and 5 nucleotides were removed from the start of forward and reverse reads, respectively (trimLeft = c(1,5)). No fixed truncation length was applied to preserve the natural length variation of the ITS2 region. Error models were learned using 1 million reads, amplicon sequence variants (ASVs) were inferred, and chimeras were removed using the consensus method.

Each ASV was taxonomically classified against the UNITE database (v8.3) using a naïve Bayes classifier in QIIME 2's feature-classifier, yielding species-level assignments where possible. The resulting abundance table containing 4,672 ASVs, taxonomy, and sample metadata (**Table S2**) was imported into phyloseq (v1.38) (McMurdie & Holmes, 2013) and merged into a single object for downstream analyses.

Initial data filtering was performed to remove low-quality or low-prevalence taxa. ASVs with a mean read count below 1×10^{-5} across all samples were removed. A prevalence filter was also applied, retaining only ASVs present in at least 5% of the samples with more than two reads. Finally, samples with fewer than 1,000 total reads were excluded, resulting in a final dataset of 1,033 ASVs across 45 samples (**Table S3**). The core microbiome, defined as the set of ASVs shared across all temperature conditions (T0, 10°C, 20°C, 30°C, and 35°C), was identified and is detailed in **Table S4**.

Alpha diversity was calculated on the filtered phyloseq object using the *estimate_richness* function from the phyloseq package. We assessed richness using Observed ASVs and diversity using the Shannon and Simpson indices. To test for significant differences in alpha diversity metrics among temperature treatments, we performed an analysis of variance (ANOVA). The normality of residuals was confirmed using the Shapiro-Wilk test. A post-hoc Tukey's Honestly Significant Difference (HSD) test was used to identify pairwise differences among temperature groups.

Beta diversity was analyzed to assess shifts in community composition. We performed a Redundancy Analysis (RDA) on a Hellinger-transformed ASV abundance matrix using the vegan package. Temperature was set as the sole constraining variable. The significance of the overall model and of each constrained axis was determined using a permutation-based ANOVA (anova.cca function with 999 permutations).

Taxonomic composition was visualized using stacked bar charts generated with ggplot2 (Wickham, 2016), showing the relative abundance of the most prevalent genera across the temperature treatments. A Venn diagram was generated using the ps_venn function to illustrate the number of shared and unique ASVs among the five temperature conditions.

Functional guild assignment was performed using FUNGuild (v1.2) (Nguyen *et al.*, 2016). The ASV table and taxonomy were used as input to assign ecological guilds to each taxon. Guild assignments were manually curated to consolidate complex or ambiguous classifications into broader, more informative categories (Saona *et al.*, 2025). Functional community structure was visualized with stacked bar charts. To test if functional profiles were significantly structured by temperature, we conducted an RDA on the Hellinger-transformed guild abundance matrix, followed by a permutational ANOVA as described for the taxonomic beta diversity.

Taxonomic identification

To identify isolates at the species level, we sequenced the internal transcribed spacer (ITS) region ITS1-5.8S-ITS2) using primers ITS1 and ITS4 (White *et al.*, 1990). DNA extraction will be performed as previously described (Villarreal *et al.*, 2022). PCR fragments will be generated using primers ITS1 and ITS4. PCR thermal profile was 96 °C 2 min, followed by 35 cycles of 96 °C for 30 s, 51 °C for 45 s, 72 °C for 120 s, and a final extension step at 72 °C for 7 min. Nucleotide sequences of the PCR products were determined by Sanger sequencing in both directions at Macrogen (Macrogen Inc., Seoul, Korea). The sequences obtained were analyzed with the PhyKit toolkit (Steenwyk *et al.*, 2021) and compared to the NCBI database using BLAST. To investigate the modulation and relationships among the species resulting from the applied temperature, phylogenetic analysis of the ITS1/ITS4 sequences of the selected isolates was performed using the R package phytools (Revell, 2024).

High-throughput physiological traits profiling

The optimum growth temperature for each isolate was obtained by measuring the thermal performance curve (TPC, the relationship between fitness-related trait performance and temperature) of its maximal growth rate at ten temperatures (12, 15, 18, 20, 25, 30, 32, 35, 37, and 40 °C) in YPD medium. For this, high-throughput phenotyping in 96-well microculture plates was performed as previously described (Villarreal *et al.*, 2022). Briefly, cells were pre-cultivated in 200 µL YPD medium without agitation at 20 °C for 48 h. For the experimental run, each well was inoculated with 10 µL of pre-inoculum to an optical density (OD_{600nm}) of 0.03-0.1 in 200 µL of YPD medium. Four independent OD measurements were taken per strain. The maximum growth rate (μ_{max}) was determined as previously described (Ibstedt *et al.*, 2015). For this, μ_{max} was calculated following a smoothing procedure on ln-transformed OD-values and using the discrete derivative, as previously described (Warringer & Blomberg, 2003, Perez-Samper *et al.*, 2018, Molinet *et al.*, 2022) in R version 4.3.1.

Modeling Thermal Performance Curves

We fitted TPCs to μ_{max} of each strain using the cardinal temperature model with inflection (CTMI) as previously described (Salvadó *et al.*, 2011, Molinet & Stelkens, 2025), using equation 1.

$$
\begin{aligned}
P &= 0 && if\ T \leq CT_{min}\ or\ T \geq CT_{max} \\
P &= P_{opt} \times \left({}^{D}/_{E}\right) && if\ CT_{min} < T < CT_{max} \\
D &= (T - CT_{max}) \times (T - CT_{min})^2 && (1) \\
E &= \left(T_{opt} - CT_{min}\right) \times \left[\left(T_{opt} - CT_{min}\right) \times \left(T - T_{opt}\right) - \left(T_{opt} - CT_{max}\right) \times \left(T_{opt} + CT_{min} - 2T\right)\right]
\end{aligned}
$$

Where:

CT_{max} is the temperature above which no growth occurs.

CT_{min} is the temperature below which no growth occurs.

T_{opt} is the temperature at which P_{max} equals its optimal value (P_{opt}).

CTMI parameters were estimated using nonlinear regression in R version 4.3.1. Thermal tolerance and Thermal breadth (T_{br}) were obtained using the calc_params function from the rTPC package (Padfield, O'Sullivan & Pawar, 2021), where thermal tolerance corresponds to CT_{max} minus $CT_{min,}$ and T_{br} is the temperature range across which performance is above 80% of optimal. The adequacy of fit of TPCs was checked by the proportion of variance explained by the model (R^2). We considered thermal parameters to differ significantly among strains if their 95% CI did not overlap. To compare TPCs between strains and to estimate the mean and 95% CI of each strain TPC, we used parametric bootstrapping, implemented in the boot package (v1.3-28.1).

Phylogenetic and non-phylogenetic comparisons

The molecular phylogeny of 12 yeast species was reconstructed from ITS sequences aligned using MAFFT v7.0. Maximum likelihood (ML) inference was performed in IQ-TREE v2.0 (Nguyen *et al.*, 2014), employing the TVMe+G4 substitution model selected via the Bayesian Information Criterion (BIC). To facilitate comparative analyses, the resulting tree was ultrametricized using penalized likelihood smoothing (Paradis, 2013) with a correlated evolutionary rate model, implemented in the R package *ape* (Paradis & Schliep, 2019).

We assessed the phylogenetic signal of six derived thermal tolerance traits (T_{min}, T_{max}, T_{opt}, P_{max}, Tolerance, and T_{br}) using three complementary metrics: Blomberg's K statistic (Blomberg, Garland & Ives, 2003), which compares observed phenotypic similarity with that expected under a Brownian motion (BM) model, where K = 1 indicates neutral evolution, K < 1 suggests evolutionary lability, and K > 1 indicates phylogenetic conservatism; (2) Pagel's λ parameter (Pagel, 1999), which assesses the degree of phylogenetic dependence of a trait, where λ = 0 indicates evolutionary independence and λ = 1 indicates Brownian evolution; and (3) Moran's I index (Gittleman & Kot, 1990), which measures the phylogenetic autocorrelation of traits (Paleo-López *et al.*, 2016, Quintero-Galvis *et al.*, 2018). The statistical significance of K and λ was assessed using 999 random permutations of trait values at the tree tips. To identify the mode of trait evolution, we compared the fit of four evolutionary models, Brownian Motion (BM), White Noise (WN), Ornstein-Uhlenbeck (OU), and Early Burst (EB), calculating Akaike weights based on sample-size corrected AIC (AICc) to determine the best-fitting model. Additionally, we visualized evolutionary trajectories through phenograms and disparity-through-time (DTT) plots. These analyses were conducted using the *phytools* (Revell, 2012) and *geiger* (Harmon *et al.*, 2008) packages in R v4.3.0.

To test for relationships between thermal traits while accounting for non-independence due to shared ancestry, we fitted PGLS models using the pgls function in the caper package (Swenson, 2014). Models incorporated thermal parameters, grouping factors, and acclimation duration as predictors, with the λ parameters estimated via maximum likelihood to control for phylogenetic signal. Finally, we replicated the signal analysis using the thermal performance curves variables (mean growth rate, mean lag phase duration, and mean maximum optical density [OD_{max}]) measured across the thermal gradient (10, 20, 30, and 35°C).

Statistical analysis

The experimental data and calculated parameters are expressed as the mean of four replicas with the corresponding standard deviation. All data were statistically analyzed with R software version 4.3.1 using a one-way ANOVA and Tukey test for mean comparisons with a *p-value* of 0.05. Heat maps were performed using the R software (Team, 2014) and the “pheatmap” package (stats 3.6.0), and plotted using the “ggplot2”

package. Principal component analysis (PCA) was performed in R software using the "prcomp" package (stat 3.6.0), and plotted with the "ggbiplot" package (Team, 2014).

Data availability statement

The data and code supporting the findings of this study are openly available at Zenodo (https://doi.org/10.5281/zenodo.18494565). Raw reads have been deposited in the Sequence Read Archive (SRA) database of the National Center for Biotechnology Information (NCBI) under the BioProject ID PRJNA1402372.

Results

Thermal stress reduces yeast richness and reshapes community composition

To evaluate the thermal resilience of the specialized yeast communities found in Sub-Antarctic soils, we exposed native samples to a controlled temperature gradient (10°C to 35°C). This experimental setup allowed us to pinpoint specific thresholds at which warming-related stress disrupts community assembly.

Incubation of sub-Antarctic soil yeast communities across a thermal gradient resulted in significant alterations in their alpha diversity (**Figure 1A-B**). Both the number of observed ASVs (richness) and the Shannon diversity index showed a clear and significant decreasing trend with increasing temperature (**Figure 1A-B**). The highest richness was recorded at the initial time point (T0), with an average of 261 ASVs (**Figure 1A**). This value remained relatively stable at 10°C and 20°C but declined significantly at 30°C (mean = 138 ASVs; Tukey's HSD, *p-value* < 0.001), and reached its minimum at 35°C (mean = 81 ASVs; *p-value* < 0.001). A similar pattern was observed for the Shannon diversity index (ANOVA, $F_{4,40}$ =8.52, *p-value* <0.001). While diversity at 10°C, 20°C, and 30°C was not statistically different from the T0 communities, the 35°C treatment caused a drastic and significant reduction in diversity compared to all other conditions (Tukey's HSD, *p-value* <0.05) (**Figure 1B**). In contrast, the Simpson diversity index did not show a statistically significant difference across treatments (ANOVA, *p-value* = 0.066), suggesting that richness and evenness declined under stress, primarily due to the loss of rare taxa, while the relative dominance of abundant taxa remained stable until the highest temperature stress was reached.

Then, to evaluate the role of temperature as a deterministic driver of community assembly, we performed a Redundancy Analysis (RDA) constrained by temperature, together with a PERMANOVA. Yeast community structure was strongly and significantly shaped by temperature (PERMANOVA, $F_{4,40}$ =2.43, *p-value* = 0.001). An RDA constrained by temperature explained 19.6% of the total variance in community composition. The first two RDA axes captured most of this constrained variance (RDA1: 59%; RDA2: 21%), clearly separating the samples along the temperature gradient (**Figure 1C**). The first axis (RDA1) primarily distinguished the extreme warming condition, separating the 35°C samples (positive scores) from the rest of the thermal gradient. The second axis (RDA2) resolved the variation among the non-extreme temperatures, separating the cold-adapted communities (Time 0 and 10°C) on the negative side from those incubated at intermediate

294 temperatures (20°C and 30°C) on the positive side. A clear taxonomic turnover drove this separation. Genera
295 such as *Pseudogymnoascus, Exophial*a, *Cortinarius*, and *Solicoccozyma* were strongly associated with the
296 cooler conditions (Time 0 and 10°C). In contrast, genera such as *Diplogelasinospora, Aspergillus*, and
297 *Humicolopsis* were highly influential in structuring communities at elevated temperatures (30°C and 35°C).
298 Overall, these results demonstrate that warming acts as a powerful deterministic filter, restructuring
299 Sub-Antarctic yeast communities. By selectively modifying the rare biosphere, which comprises specialized
300 cold-adapted taxa, while favoring a resilient group of persistent residents, thermal stress drives a non-uniform
301 erosion of diversity. This selective sorting process shapes niche occupation along the thermal gradient,
302 triggering profound taxonomic turnover that replaces historically stable cold-associated assemblages with
303 thermotolerant groups.
304

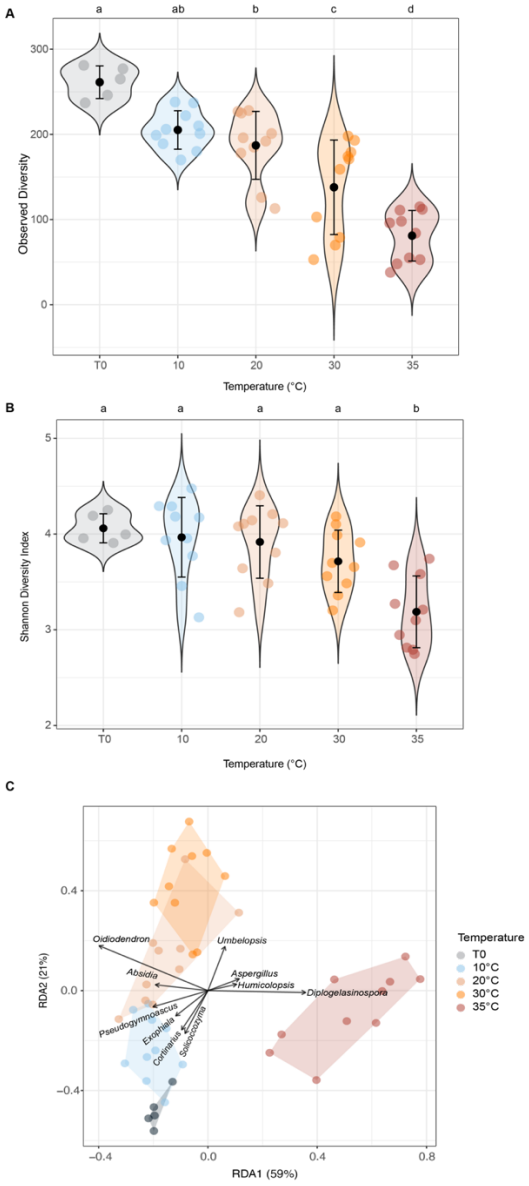

Figure 1. Effects of temperature on yeast community diversity and structure. (A) Observed diversity (number of ASVs) and (B) Shannon diversity index across the temperature gradient (Time 0, 10°C, 20°C, 30°C, and 35°C). Letters above the violin plots indicate significant differences between groups based on a Tukey's HSD post-hoc test (*p-value* <0.05). The central black bar represents the standard deviation of the distribution around the mean. (C) Redundancy Analysis (RDA) of Hellinger-transformed yeast community composition constrained by temperature. Points represent individual samples, colored by temperature treatment. Polygons enclose all samples from a given treatment. Arrows indicate the top 10 most influential genera driving the community separation. The percentage of variance explained by each axis is shown in parentheses.

Taxonomic and functional profiles shift towards warm-associated taxa

The shift in community structure was reflected in the overall taxonomic profiles at the genus level (**Figure 2A**). While the initial T0 community was diverse, warming induced a progressive shift towards a community heavily dominated by *Diplogelasinospora* at 35°C. A Venn diagram analysis revealed that despite this turnover, a core microbiome of 114 ASVs was shared across all temperature conditions (**Figure S2, Table S4**).

An analysis of these 114 core taxa showed that temperature was also associated with consistent changes within this stable portion of the community (**Figure S2A, Table S4**). Core members of genera such as *Pseudogymnoascus* and *Penicillium* were abundant at lower temperatures but declined in relative abundance under warming conditions. Conversely, core taxa from genera like *Humicolopsis* and *Absidia*, while present initially, increased in relative abundance at 30°C and 35°C (**Figure S2B**). These patterns indicate that temperature influenced the relative contributions of taxa even within the shared core community. Functionally, yeast communities were dominated by Saprotrophs and Wood Saprotrophs across all temperatures (**Figure 2B**), although the relative proportions of other guilds shifted along the thermal gradient. Ectomycorrhizal fungi, present in the T0 and 10°C treatments, were nearly absent at 30°C and 35°C. Consistently, the RDA based on functional guild profiles showed that temperature significantly structured community functional profiles (PERMANOVA, $F_{4,40}$ = 3.50, *p-value* = 0.001), explaining 18.5% of the variance (**Figure 2C**). Lower temperature communities were associated with Ectomycorrhizal guilds, whereas higher temperatures were associated with increased contributions of Saprotroph and Wood Saprotroph functions.

Overall, these results show that increasing temperature was associated with coordinated shifts in both taxonomic composition and functional profiles of yeast communities. Changes in genus-level dominance, functional guild composition, and relative abundances within a shared core microbiome were consistent along the thermal gradient.

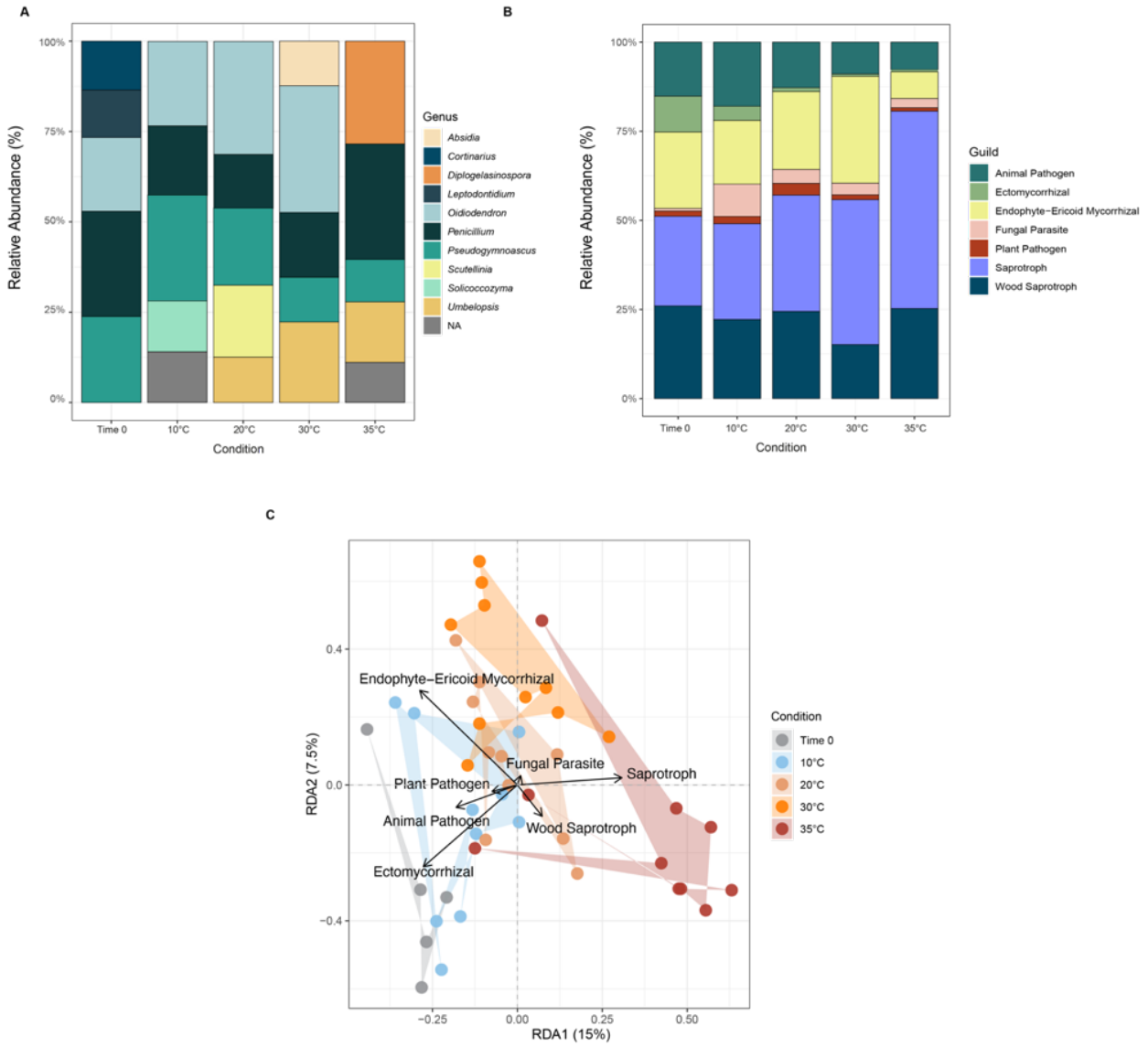

Figure 2. Taxonomic and functional shifts in yeast communities under thermal gradient. (A) Relative abundance of the most prevalent fungal genera across all temperature treatments. (B) Relative abundance of functional guilds, assigned by FUNGuild, across the temperature gradient. (C) Redundancy Analysis (RDA) of Hellinger-transformed functional guild profiles constrained by temperature, with arrows indicating the major guilds driving community separation.

Thermal sorting reveals hidden yeast diversity

To establish a mechanistic link between taxonomic turnover and individual physiological traits, we complemented our molecular analysis with a detailed characterization of the culturable yeast assemblages (**Figure S1, Figure 3**). This culture-dependent approach was essential for distinguishing between the environmental presence of DNA sequences and the metabolic viability of the constituent taxa. By isolating yeasts from microcosms across the thermal gradient (10°C to 35°C), we were able to directly assess whether the shifts observed in the molecular data correspond to the resuscitation and active growth of thermotolerant lineages from the seed bank. Samples obtained from tubes exposed to increasing sorting temperatures (10°C, 20°C, 30°C, and 35°C) were incubated under two conditions: (i) at the same temperature used for sorting, and (ii) under a control incubation at 20°C (**Figures S1**, **Figure 3**). This approach allowed us to distinguish between two ecological responses: the ability of yeasts to tolerate a transient exposure to elevated temperature during the sorting process, and their capacity to maintain active growth and reproduction under sustained warming conditions.

At time 0, following incubation at 20°C, culturable yeasts recovered from rhizosphere soils of the Karukinka Natural Park revealed a diverse assemblage of ten species, including *Solicoccozyma aeria*, *Solicoccozyma terreus*, *Saitozyma podzolica*, *Coniochaeta lignaria*, *Teunomyces cretensis*, *Meyerozyma guilliermondii*, *Candida boleticola*, *Holtarmanniella wattica*, *Trichosporon japonicum*, and *Candida sake* (**Figure 3**). This assemblage comprised both basidiomycetous and ascomycetous yeasts, encompassing taxa typically associated with cold, organic-rich soils, plant-associated niches, and decomposer lifestyles. The recovery of this taxonomically and ecologically heterogeneous culturable community from the rhizosphere establishes a baseline diversity before thermal filtering. It provides a reference point for evaluating temperature-driven shifts in yeast composition and growth performance.

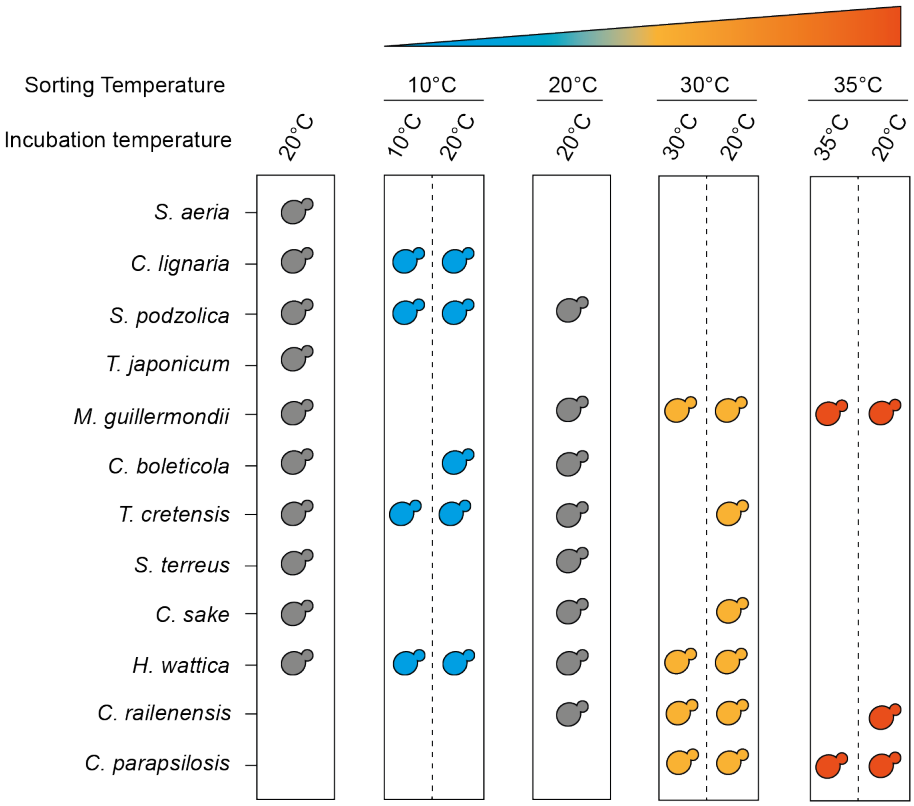

Figure 3. Thermal sorting reveals latent diversity within sub-Antarctic yeast communities. Yeast species isolated from soil samples subjected to sorting at increasing temperatures (10°C, 20°C, 30°C, and 35°C) and subsequently incubated either at the same temperature (Sorting Temperature) or under control conditions (20°C).

After sorting, the composition of culturable yeasts showed a clear non-random pattern along the thermal gradient (**Figure 3, Table S5)**. Low-temperature treatments (10 °C and 20 °C) were dominated by taxa such as *C. lignaria*, *T. cretensis,* and *S. podzolica*. These species exhibited a stenothermal response, showing reduced recovery as temperatures increased and complete exclusion at 35 °C. In contrast, some taxa, such as *H. wattica*, displayed remarkable thermal plasticity, persisting across intermediate and high-temperature regimes (10-30 °C). Interestingly, *C. sake* and *T. cretensis* were recovered after sorting at 30 °C, but only when cultivated at 20 °C, highlighting their ability to tolerate incubation at 30 °C rather than to grow at that temperature. *M. guillermondii* exhibits an exceptional resilience to warming conditions, being isolated from conditions ranging from 20 °C to 35 °C (**Figure 3, Table S4**). These results suggest that these species possess broader thermal niches, allowing them to maintain activity as the environment warms.

Finally, the thermal sorting process revealed a fraction of "hidden" yeast diversity that was undetectable in the baseline community. This emergence followed two distinct patterns. First, *Candida railenensis* appeared as a latent taxon with a broad thermal niche. This species was successfully isolated from soils incubated at 20-35 °C, suggesting it is a rare biosphere member that thrives when competitive pressure from cold-adapted specialists is removed. Second, in contrast to this broad emergence, *Candida parapsilosis* exhibited a strict high-temperature requirement, being exclusively retrieved at the most extreme conditions of 30 and 35 °C. This specific recruitment of latent taxa drove marked compositional turnover at the genus level (**Figure S3**). The relative contribution of *Candida* species to the culturable community increased progressively along the thermal gradient. While Candida isolates constituted a minor fraction at lower temperatures (20% at 10 °C), their prevalence increased under warming conditions, ultimately making them the dominant group at 35 °C, where they represented 67% of the recovered isolates (**Figure S3**).

Together, these results indicate that warming does not simply reduce diversity; it reorders the community by filtering out cold specialists and "unlocking" a cryptic reservoir of thermotolerant species, such as *Candida* spp*.,* that occupy distinct thermal niches, from the broadly adaptable *C. railenensis* to the heat-specialized *C. parapsilosis*.

Yeast species display extensive variation in thermal performance across a temperature gradient

To determine whether the temperature-dependent shifts observed in the cultivable yeast community were associated with intrinsic differences in thermal tolerance and growth capacity, we quantified thermal performance curves (TPCs) for all recovered yeast species across a broad temperature gradient (**Figure S4**). This approach allowed us to link community-level sorting patterns (**Figure 3**) to species-specific traits, including optimum growth temperature (T_{opt}), maximum growth rate (P_{max}), and thermal breadth (**Table S6**).

The TPC profiling revealed a stark physiological divergence that mirrors the ecological turnover. Species that were filtered out by warming, such as *S. podzolica*, *S. aeria*, and *C. sake*, exhibited significantly lower thermal optima (T_{opt} < 25 °C) (**Figure 4A, Table S6**). Their performance curves declined abruptly beyond

this threshold (**Figure S4**), providing a mechanistic explanation for their inability to persist at 30 °C and 35 °C. In contrast, the taxa that dominated under warming displayed distinct warm-adapted signatures. *M. guilliermondii* and *C. parapsilosis* exhibited the highest thermal optima of the assemblage, with T_{opt} values reaching approximately 40 °C and 32°C, respectively (**Figure 4, Table S5**). This high thermal preference explains their competitive advantage and dominance at the upper end of the experimental gradient.

Analysis of maximum growth (P_{max}) revealed that thermal dominance was not strictly coupled with growth speed (**Figure 4B**). While *H. wattica* exhibited the highest potential growth rate of the entire community (μ_{max} = 0.25 OD/h), its lower T_{opt} (< 30 °C) limited its success under extreme warming. Meanwhile, the dominant *Candida* species at high temperatures maintained moderate but sustained growth rates. This suggests that in this system, having a compatible thermal niche is a stronger predictor of persistence than peak growth potential alone.

Finally, the shape of the thermal curves highlighted contrasting survival strategies among the warm-tolerant taxa (**Figure 4C**). *C. railenensis* displayed one of the widest thermal breadths (> 12 °C). This broad physiological plasticity supports its characterization as a thermal generalist, capable of maintaining high performance across the shifting conditions from 20 °C to 35 °C. Conversely, and surprisingly given its wide ecological recovery, *M. guilliermondii* exhibited the narrowest thermal breadth of the isolates (7 °C) (**Figure 4C**), similar to the cold-stenotherm *S. podzolica*. Coupled with its high T_{opt}, this profile indicates that *M. guilliermondii* is a warm-specialist. Its presence at lower temperatures (20 °C) in the sorting experiments likely reflects a capacity for sub-optimal survival rather than broad physiological adaptation. In contrast, its explosive dominance at 35 °C aligns with its specialized peak performance.

Collectively, these physiological fingerprints confirm that the community reordering was not stochastic. Warming acted as a filter, selecting for two distinct warm-response strategies: the plastic generalism of *C. railenensis* and the high-temperature specialization of *M. guilliermondii* and *C. parapsilosis*.

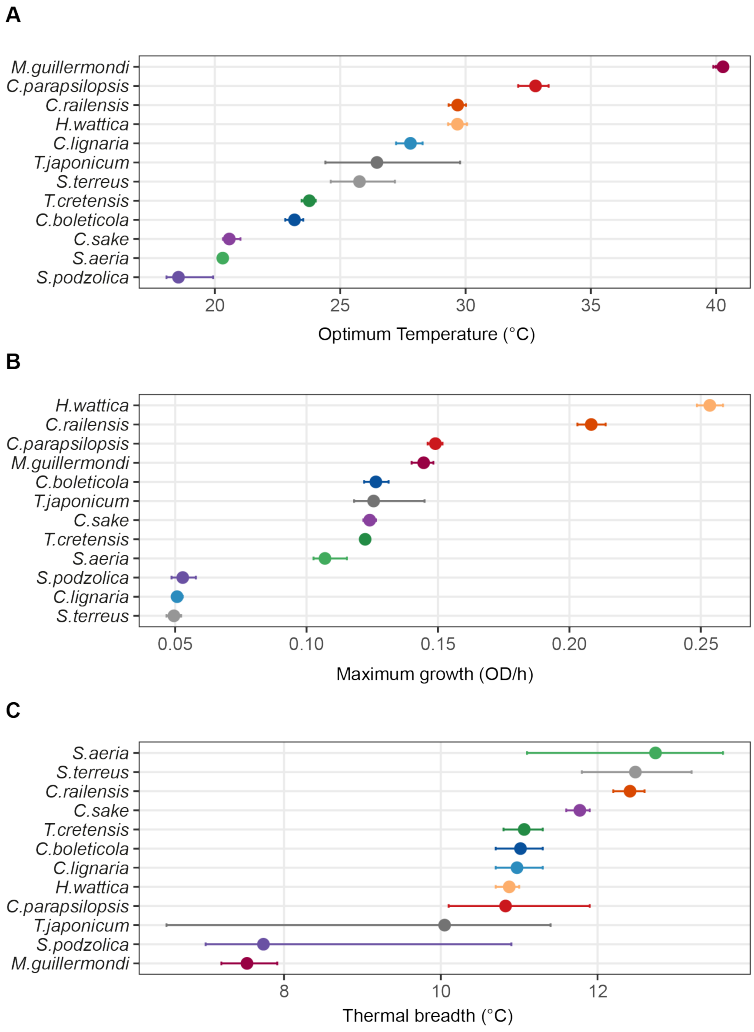

Figure 4. Thermal performance profiles of yeast species isolated from sub-Antarctic soils. (A) Optimum growth temperature (T_{opt}) calculated from fitted thermal performance curves. (B) The maximum growth rate (P_{max}) was obtained for each species. (C) Thermal breadth, defined as the temperature range over which each species maintained at least 80% of its maximum growth rate.

Reduced phylogenetic structuring reflects environment-driven thermal traits

Phylogenetic signal analyses revealed a consistent absence of phylogenetic structure in all assessed thermal parameters (**Table S6**). Blomberg's K statistic was extremely low and not significant for any trait ($K = 0.041$, $p > 0.41$ in all cases), indicating that the similarity between closely related species is much lower than expected under a Brownian evolution model. Consistently, Pagel's λ parameter was practically zero for all traits ($\lambda < 0.001$, $p = 1.00$ for T_{max}, Thermal Breadth, Tolerance, T_{min}, and T_{opt}; $\lambda = 0$ for P_{max}), suggesting that phylogeny does not explain the observed variation in thermal tolerances. Moran's I index confirmed this pattern, with

low and mostly non-significant values (I = 0.037–0.171, p > 0.09), except for T_{min} (I = 0.171, p = 0.028) (**Figure S5A**) and P_{max} (I = 0.350, p < 0.001), which showed a weak but significant positive phylogenetic autocorrelation (**Figure S5C**).

Comparison of evolutionary models provided conclusive evidence that thermal traits evolve independently of phylogenetic history. The White Noise model fit substantially better than the Brownian model for all traits, with Akaike weights greater than 98% for five of the six traits analyzed (T_{max} = 100.0%, Thermal Breadth = 98.6%, tolerance = 98.8%, T_{min} = 98.5%, T_{opt} = 99.9%). Only P_{max} showed moderate support for the White Noise model (weight = 28.7%), although this remained the highest-ranked model. The differences in AICc between models (ΔAICc = 50.8–100.8) indicate that the phylogenetic models (Brownian Motion, Ornstein-Uhlenbeck, Early Burst) are substantially less plausible than the independent evolution model. PGLS models confirmed the absence of phylogenetic structure in trait relationships ($\lambda < 0.05$ in all models). T_{min} showed a significant positive relationship with T_{max} ($\beta = 0.65$, $t = 5.4$, $p < 0.001$), independent of phylogeny. The results were qualitatively identical using ordinary linear regression ($\beta = 0.68$, $p < 0.001$), validating that the relationships are not confounded by shared evolutionary history.

Phylogenetic signal analyses of three growth curve traits (growth rate, lag phase, and maximum optical density) evaluated at four temperatures (10, 20, 30, and 35°C) revealed a generalized absence of phylogenetic structure under most thermal conditions (**Table S7**). Even under cold stress (10 °C), K = 0.239–0.371 and Pagel λ values ($\lambda \leq 0.001$) remained non-significant ($P > 0.07$). However, the maximum optical density (mean OD_{max}) at 10 °C showed a unique trend: it was the only instance where the Brownian model marginally outperformed White Noise, suggesting a weak phylogenetic constraint on biomass production under cold conditions. Conversely, at optimal (20 °C) and heat-stress (30–35 °C) temperatures, phylogenetic signal was completely absent, confirming that physiological responses to warming evolve independently across lineages.

Discussion

Our findings demonstrate that warming acts as a potent deterministic filter in Sub-Antarctic soils, fundamentally reshaping yeast communities by unlocking a cryptic reservoir of thermotolerant taxa. This shift is characterized by a significant decline in alpha diversity and a clear, temperature-dependent separation in community composition (RDA and PERMANOVA), indicating that thermal stress reduces richness primarily by excluding rare, cold-adapted taxa. Such a pattern provides direct evidence for the species-sorting paradigm, in which environmental stressors act as deterministic filters that select for taxa with thermal tolerance (He *et al.*, 2021, Chen *et al.*, 2022, Litchman & Thomas, 2022, Smith *et al.*, 2022). While temperature is a universal constraint on microbial metabolism (Delgado-Baquerizo *et al.*, 2016, Berdugo *et al.*, 2018), our results underscore that in historically stable Sub-Antarctic ecosystems, it triggers an abrupt taxonomic turnover that favors opportunistic lineages, most notably within the genus *Candida*, as long-standing thermal barriers are breached.

In line with the expected outcome that thermal niches would dictate community structure, the observed taxonomic turnover confirms that warming acts as a precise deterministic filter. While we expected cold-adapted residents to dominate the baseline conditions, their systematic replacement by thermotolerant opportunists at higher temperatures provides a clear view of species sorting in action. At lower temperatures, the community was indeed characterized by psychrotolerant taxa such as *Cortinarius* and *Solicoccozyma*, typical of cold high-latitude soils (Timling *et al.*, 2014, Treseder & Lennon, 2015, Saona *et al.*, 2025). Conversely, as temperature increased, we observed a shift toward *Diplogelasinospora* and Aspergillus, which became dominant due to their faster growth and greater resource utilization under thermal stress (Delgado-Baquerizo *et al.*, 2018). Our culture-dependent physiological profiling confirms the mechanistic basis for what was seen in the metabarcoding: the rapid exclusion of cold-associated species like *S. podzolica* and *S. aeria* is directly explained by their physiological constraints, such as sharp performance declines and low T_{opt} (< 25 °C). These findings validate our prediction that thermal sensitivity is a conserved microbial trait that dictates community boundaries under climate change (Alster, Weller & von Fischer, 2018, Molinet & Stelkens, 2025).

While these results provide critical insights, it is important to acknowledge the inherent methodological biases associated with yeast isolation. The selection of specific culture conditions may influence the observed proportions and diversity of culturable species, as not all taxa may be equally recoverable in the laboratory. Nonetheless, the strong congruence between our physiological data and broader molecular patterns suggests that these isolates serve as a robust proxy for the community's response to warming.

The divergence in physiological strategies among the emerging dominant taxa reveals a sophisticated mechanism of niche occupancy within the cryptic reservoir. Rather than a uniform response to heat, the "unlocking" of this hidden diversity relies on a dual pathway: niche expansion by plastic generalists such as *C. railenensis* and competitive exclusion at high-temperature peaks by specialists such as *M. guilliermondii* and *C. parapsilosis*. This multi-faceted response suggests that the Sub-Antarctic microbial seed bank is pre-adapted to a variety of warming scenarios, from gradual shifts to extreme heat events. While generalists provide the community with initial flexibility to colonize newly available thermal spaces, specialists ensure dominance once thermal thresholds are breached, effectively out-competing cold-adapted residents. Such a combination of thermal breadth and performance limits explains why warming-induced assembly is so rapid and difficult to reverse, as these taxa do not merely survive the heat, they are physiologically primed to exploit it (Boixel *et al.*, 2019, Wieczynski *et al.*, 2021).

A critical finding of this study is that extreme warming unlocked a cryptic reservoir of yeast diversity undetectable under ambient conditions. The emergence of *Candida* species at 30 °C and 35 °C, taxa likely belonging to the rare biosphere at lower temperatures, supports the hypothesis that soils harbor latent functional diversity capable of responding rapidly to fluctuations (Smith *et al.*, 2022). These conditionally rare taxa likely persist in low abundance or dormancy within the cold sub-Antarctic soil, providing a "seed bank" for ecosystem resilience (Jansson & Hofmockel, 2020, Eisenhauer *et al.*, 2023). However, this effect comes at a cost: the awakening of this reservoir led to a marked homogenization of the culturable community, shifting from a diverse assemblage to one heavily dominated by opportunistic *Candida* species. This transition suggests that while functional processes might be maintained, the phylogenetic structure and functional

redundancy of the community could be compromised under sustained warming (Eisenhauer *et al.*, 2023, Ramond, Galand & Logares, 2025).

The marked dominance of *Candida* species in our warming microcosms provides empirical evidence for the ongoing erosion of the mammalian thermal barrier (Garcia-Solache & Casadevall, 2010, Robert, Cardinali & Casadevall, 2015). According to the hypothesis proposed by Casadevall, the endothermic nature of mammals (37 °C) has historically served as a robust evolutionary shield against most environmental fungi (Casadevall, 2012). However, our results demonstrate that anthropogenic warming exerts selective pressure, training environmental assemblages to tolerate higher thermal optima (Casadevall, Kontoyiannis & Robert, 2019, Nnadi & Carter, 2021). This process effectively narrows the thermal gap between the environment and endothermic hosts (Smith *et al.*, 2025).

Finally, the absence of phylogenetic signals in thermal tolerance traits and growth curve parameters suggests that these characters are evolutionarily highly labile and respond more to local selective pressures than to the conservation of ancestral values. This pattern contrasts with the widely documented expectation of thermal niche conservatism in other taxa (Wiens *et al.*, 2010), where closely related species are expected to maintain similar physiological phenotypes inherited from common ancestors. Our results suggest that the yeast species examined in this study possess an exceptional capacity to adapt their thermal limits to the environmental conditions of their current habitats. The independent evolution of T_{min}, T_{max}, and T_{opt} among lineages implies that closely related species can occupy dramatically different thermal niches, likely reflecting an ability to adapt to microhabitats with different thermal regimes, phenotypic plasticity, or divergent selection along different thermal gradients (Buckley & Kingsolver, 2021). Each lineage has independently optimized its growth rate, acclimation lag, and ability to reach high biomass (OD_{max}) in response to the specific thermal conditions of its current ecological niche. The weak signal detected in P_{max} could indicate conserved physiological limitations in the underlying metabolic machinery, while the upper and lower thermal limits are more plastic. This evolutionary lability has important implications for predicting responses to climate change, suggesting that the analyzed species may have a greater capacity for rapid evolutionary responses to new

thermal regimes than taxa with conserved thermal niches. The independent evolution of thermal tolerances has likely facilitated the coexistence of related species across environmental gradients, allowing for the partitioning of thermal resources (e.g., specialization in warm vs. cold microhabitats within the same ecosystem).

Overall, our findings highlight temperature as a central deterministic driver of microbial community assembly in Sub-Antarctic soils. By filtering cold-specialized taxa and promoting the resuscitation of thermotolerant lineages from the rare biosphere, warming reshapes yeast diversity and selects for specific life-history strategies. The transition from complex, cold-adapted communities to simplified assemblages dominated by opportunistic generalists could have profound implications for soil processes, including decomposition rates and nutrient turnover (Zhou *et al.*, 2023). Moreover, we hypothesize that the selective proliferation of these thermotolerant opportunistic lineages under sustained warming may expand the environmental reservoir of emerging fungal pathogens, potentially posing new health risks to resident biota and wildlife as historical thermal barriers are breached. Understanding this thermally driven restructuring and the physiological mechanisms behind it is essential for predicting the functional trajectory of high-latitude ecosystems in a warming world.

Acknowledgments

We would like to express our sincere gratitude to Francisco A. Cubillos for his support during sampling and for his insightful advice and feedback throughout the development of this study. We also thank Valentina Abarca and Matias Castillo for their technical support. This research was funded by Agencia Nacional de Investigación y Desarrollo (ANID) FONDECYT Iniciación (11240649) and ANID - Programa Iniciativa Científica Milenio ICN17_022 and NCN2021_050. LAS acknowledges ANID Postdoctoral FONDECYT [3240351]. JM was funded by ANID FONDECYT Iniciación grant 11260235. We acknowledge Fundación Ciencia & Vida for providing infrastructure, laboratory space, and equipment for experiments. The graphical abstract was generated using the artificial intelligence model Gemini.

Author Contributions

Conceptualization: JM and PV. **Formal analysis:** LAS, MLHP, JBP, FJ, JFQG, JM, and PV. **Investigation:** LAS, JFQG, JM, and PV. **Writing–original draft:** LS, JM, and PV. **Writing – review & editing:** LAS, JFQG, JM, and PV.

Conflict of interest

The authors declare no conflicts of interest.

References

Abs E, Chase AB & Allison SD (2023) How do soil microbes shape ecosystem biogeochemistry in the context of global change? *Environ Microbiol* **25**: 780-785.

Allison SD & Martiny JBH (2008) Resistance, resilience, and redundancy in microbial communities. *Proceedings of the National Academy of Sciences* **105**: 11512-11519.

Alster CJ, Weller ZD & von Fischer JC (2018) A meta-analysis of temperature sensitivity as a microbial trait. *Glob Chang Biol* **24**: 4211-4224.

Barnes-Keoghan I & Pendlebury S (2023) Climate and climate change in the sub-Antarctic.

Berdugo M, Maestre FT, Kéfi S, Gross N, Le Bagousse-Pinguet Y, Soliveres S & Gomez-Aparicio L (2018) Aridity preferences alter the relative importance of abiotic and biotic drivers on plant species abundance in global drylands. *Journal of Ecology* **107**: 190-202.

Blomberg SP, Garland T, Jr. & Ives AR (2003) Testing for phylogenetic signal in comparative data: behavioral traits are more labile. *Evolution* **57**: 717-745.

Boixel AL, Delestre G, Legeay J, Chelle M & Suffert F (2019) Phenotyping Thermal Responses of Yeasts and Yeast-like Microorganisms at the Individual and Population Levels: Proof-of-Concept, Development and Application of an Experimental Framework to a Plant Pathogen. *Microb Ecol* **78**: 42-56.

Bolyen E & Rideout JR & Dillon MR*, et al.* (2019) Reproducible, interactive, scalable and extensible microbiome data science using QIIME 2. *Nature Biotechnology* **37**: 852-857.

Buckley LB & Kingsolver JG (2021) Evolution of Thermal Sensitivity in Changing and Variable Climates. *Annual Review of Ecology, Evolution, and Systematics* **52**: 563-586.

Burman E & Bengtsson-Palme J (2021) Microbial Community Interactions Are Sensitive to Small Changes in Temperature. *Front Microbiol* **12**: 672910.

Callahan BJ, McMurdie PJ, Rosen MJ, Han AW, Johnson AJA & Holmes SP (2016) DADA2: High-resolution sample inference from Illumina amplicon data. *Nature Methods* **13**: 581-583.

Casadevall A (2012) Fungi and the Rise of Mammals. *PLOS Pathogens* **8**: e1002808.

Casadevall A, Kontoyiannis Dimitrios P & Robert V (2019) On the Emergence of Candida auris: Climate Change, Azoles, Swamps, and Birds. *mBio* **10**: 10.1128/mbio.01397-01319.

Casadevall A, Kontoyiannis DP & Robert V (2019) On the Emergence of Candida auris: Climate Change, Azoles, Swamps, and Birds. *mBio* **10**: 10.1128/mbio.01397-01319.

Cavicchioli R, Ripple WJ, Timmis KN*, et al.* (2019) Scientists' warning to humanity: microorganisms and climate change. *Nature Reviews Microbiology* **17**: 569-586.

Chen H, Chen Z, Chu X, Deng Y, Qing S, Sun C, Wang Q, Zhou H, Cheng H, Zhan W & Wang Y (2022) Temperature mediated the balance between stochastic and deterministic processes and reoccurrence of microbial community during treating aniline wastewater. *Water Res* **221**: 118741.

Delgado-Baquerizo M, Reith F, Dennis PG, Hamonts K, Powell JR, Young A, Singh BK & Bissett A (2018) Ecological drivers of soil microbial diversity and soil biological networks in the Southern Hemisphere. *Ecology* **99**: 583-596.

Delgado-Baquerizo M, Maestre FT, Reich PB, Jeffries TC, Gaitan JJ, Encinar D, Berdugo M, Campbell CD & Singh BK (2016) Microbial diversity drives multifunctionality in terrestrial ecosystems. *Nat Commun* **7**: 10541.
Delgado-Baquerizo M, Oliverio AM, Brewer TE, Benavent-González A, Eldridge DJ, Bardgett RD, Maestre FT, Singh BK & Fierer N (2018) A global atlas of the dominant bacteria found in soil. *Science* **359**: 320-325.
Diaz-Colunga J, Lu N, Sanchez-Gorostiaga A, Chang CY, Cai HS, Goldford JE, Tikhonov M & Sanchez A (2022) Top-down and bottom-up cohesiveness in microbial community coalescence. *Proc Natl Acad Sci U S A* **119**.
Eisenhauer N, Hines J, Maestre FT & Rillig MC (2023) Reconsidering functional redundancy in biodiversity research. *NPJ Biodivers* **2**: 9.
Garcia-Solache MA & Casadevall A (2010) Global Warming Will Bring New Fungal Diseases for Mammals. *mBio* **1**: 10.1128/mbio.00061-00010.
Gittleman JL & Kot M (1990) Adaptation: Statistics and a Null Model for Estimating Phylogenetic Effects. *Systematic Biology* **39**: 227-241.
Harmon LJ, Weir JT, Brock CD, Glor RE & Challenger W (2008) GEIGER: investigating evolutionary radiations. *Bioinformatics* **24**: 129-131.
He Q, Wang S, Hou W, Feng K, Li F, Hai W, Zhang Y, Sun Y & Deng Y (2021) Temperature and microbial interactions drive the deterministic assembly processes in sediments of hot springs. *Sci Total Environ* **772**: 145465.
Ibstedt S, Stenberg S, Bagés S*, et al.* (2015) Concerted evolution of life stage performances signals recent selection on yeast nitrogen use. *Mol Biol Evol* **32**: 153-161.
Intergovernmental Panel on Climate C (2023) *Climate Change 2021 – The Physical Science Basis: Working Group I Contribution to the Sixth Assessment Report of the Intergovernmental Panel on Climate Change*. Cambridge University Press, Cambridge.
Jansson JK & Hofmockel KS (2020) Soil microbiomes and climate change. *Nat Rev Microbiol* **18**: 35-46.
Knight CG, Nicolitch O, Griffiths RI*, et al.* (2024) Soil microbiomes show consistent and predictable responses to extreme events. *Nature* **636**: 690-696.
Litchman E & Thomas MK (2022) Are we underestimating the ecological and evolutionary effects of warming? Interactions with other environmental drivers may increase species vulnerability to high temperatures. *Oikos* **2023**.
McMurdie PJ & Holmes S (2013) phyloseq: An R Package for Reproducible Interactive Analysis and Graphics of Microbiome Census Data. *PLOS ONE* **8**: e61217.
Meir P, Cox P & Grace J (2006) The influence of terrestrial ecosystems on climate. *Trends in Ecology & Evolution* **21**: 254-260.
Molinet J & Stelkens R (2025) The evolution of thermal performance curves in response to rising temperatures across the model genus yeast. *Proceedings of the National Academy of Sciences* **122**: e2423262122.
Molinet J, Urbina K, Villegas C, Abarca V, Oporto CI, Villarreal P, Villarroel CA, Salinas F, Nespolo RF & Cubillos FA (2022) A Saccharomyces eubayanus haploid resource for research studies. *Scientific Reports* **12**: 5976.

Nguyen L-T, Schmidt HA, von Haeseler A & Minh BQ (2014) IQ-TREE: A Fast and Effective Stochastic Algorithm for Estimating Maximum-Likelihood Phylogenies. *Molecular Biology and Evolution* **32**: 268-274.
Nguyen NH, Song Z, Bates ST, Branco S, Tedersoo L, Menke J, Schilling JS & Kennedy PG (2016) FUNGuild: An open annotation tool for parsing fungal community datasets by ecological guild. *Fungal Ecology* **20**: 241-248.
Nnadi NE & Carter DA (2021) Climate change and the emergence of fungal pathogens. *PLOS Pathogens* **17**: e1009503.
Padfield D, O'Sullivan H & Pawar S (2021) rTPC and nls.multstart: A new pipeline to fit thermal performance curves in r. *Methods in Ecology and Evolution* **12**: 1138-1143.
Pagel M (1999) Inferring the historical patterns of biological evolution. *Nature* **401**: 877-884.
Paleo-López R, Quintero-Galvis JF, Solano-Iguaran JJ, Sanchez-Salazar AM, Gaitan-Espitia JD & Nespolo RF (2016) A phylogenetic analysis of macroevolutionary patterns in fermentative yeasts. *Ecology and Evolution* **6**: 3851-3861.
Paradis E (2013) Molecular dating of phylogenies by likelihood methods: a comparison of models and a new information criterion. *Mol Phylogenet Evol* **67**: 436-444.
Paradis E & Schliep K (2019) ape 5.0: an environment for modern phylogenetics and evolutionary analyses in R. *Bioinformatics* **35**: 526-528.
Pendlebury S & Barnes-Keoghan IP (2007) Climate and climate change in the sub-Antarctic. *Papers and Proceedings of the Royal Society of Tasmania* 67-81.
Perez-Samper G, Cerulus B, Jariani A*, et al.* (2018) The Crabtree Effect Shapes the Saccharomyces cerevisiae Lag Phase during the Switch between Different Carbon Sources. *mBio* **9**.
Quintero-Galvis JF, Paleo-López R, Solano-Iguaran JJ, Poupin MJ, Ledger T, Gaitan-Espitia JD, Antoł A, Travisano M & Nespolo RF (2018) Exploring the evolution of multicellularity in Saccharomyces cerevisiae under bacteria environment: An experimental phylogenetics approach. *Ecology and Evolution* **8**: 4619-4630.
Ramond P, Galand PE & Logares R (2025) Microbial functional diversity and redundancy: moving forward. *FEMS Microbiol Rev* **49**.
Revell LJ (2012) phytools: an R package for phylogenetic comparative biology (and other things). *Methods in Ecology and Evolution* **3**: 217-223.
Revell LJ (2024) phytools 2.0: an updated R ecosystem for phylogenetic comparative methods (and other things). *PeerJ* **12**: e16505.
Robert V, Cardinali G & Casadevall A (2015) Distribution and impact of yeast thermal tolerance permissive for mammalian infection. *BMC Biol* **13**: 18.
Rodriguez Amor D & Dal Bello M (2019) Bottom-Up Approaches to Synthetic Cooperation in Microbial Communities. *Life (Basel)* **9**.
Runnel K, Tedersoo L, Krah FS, Piepenbring M, Scheepens JF, Hollert H, Johann S, Meyer N & Bassler C (2025) Toward harnessing biodiversity-ecosystem function relationships in fungi. *Trends Ecol Evol* **40**: 180-190.
Salvadó Z, Arroyo-López FN, Guillamón JM, Salazar G, Querol A & Barrio E (2011) Temperature adaptation markedly determines evolution within the genus Saccharomyces. *Appl Environ Microbiol* **77**: 2292-2302.

Saona LA, Oporto CI, Villarreal P, Urbina K, Correa C, Quintero-Galvis JF, Moreno-Meynard P, Piper FI, Vianna JA, Nespolo RF & Cubillos FA (2025) High ectomycorrhizal relative abundance during winter at the treeline. *ISME Commun* **5**: ycaf010.
Smith DFQ, Kulkarni M, Bencomo A, Faiez TS, Hardwick JM & Casadevall A (2025) Environmental fungi from cool and warm neighborhoods in the heat island of Baltimore City show differences in thermal susceptibility and pigmentation. *ISME Communications* **5**.
Smith TP, Mombrikotb S, Ransome E, Kontopoulos DG, Pawar S & Bell T (2022) Latent functional diversity may accelerate microbial community responses to temperature fluctuations. *eLife* **11**: e80867.
Steenwyk JL, Buida TJ, Labella AL, Li Y, Shen XX & Rokas A (2021) PhyKIT: a broadly applicable UNIX shell toolkit for processing and analyzing phylogenomic data. *Bioinformatics* **37**: 2325-2331.
Swenson NG (2014) *Functional and Phylogenetic Ecology in R*. Springer New York.
Team TRC (2014) R: A Language and Environment for Statist.
Timling I, Walker DA, Nusbaum C, Lennon NJ & Taylor DL (2014) Rich and cold: diversity, distribution and drivers of fungal communities in patterned-ground ecosystems of the North American Arctic. *Mol Ecol* **23**: 3258-3272.
Treseder KK & Lennon JT (2015) Fungal traits that drive ecosystem dynamics on land. *Microbiol Mol Biol Rev* **79**: 243-262.
Villarreal P, Quintrel PA, Olivares-Munoz S, Ruiz JJ, Nespolo RF & Cubillos FA (2022) Identification of new ethanol-tolerant yeast strains with fermentation potential from central Patagonia. *Yeast* **39**: 128-140.
Warringer J & Blomberg A (2003) Automated screening in environmental arrays allows analysis of quantitative phenotypic profiles in Saccharomyces cerevisiae. *Yeast* **20**: 53-67.
White TJ, Bruns T, Lee S & Taylor J (1990) 38 - AMPLIFICATION AND DIRECT SEQUENCING OF FUNGAL RIBOSOMAL RNA GENES FOR PHYLOGENETICS. *PCR Protocols,*(Innis MA, Gelfand DH, Sninsky JJ & White TJ, eds.), p.^pp. 315-322. Academic Press, San Diego.
Wickham H (2016) Programming with ggplot2. *ggplot2: Elegant Graphics for Data Analysis,*(Wickham H, ed.) p.^pp. 241-253. Springer International Publishing, Cham.
Wieczynski DJ, Singla P, Doan A, Singleton A, Han ZY, Votzke S, Yammine A & Gibert JP (2021) Linking species traits and demography to explain complex temperature responses across levels of organization. *Proc Natl Acad Sci U S A* **118**.
Wiens JJ, Ackerly DD, Allen AP*, et al.* (2010) Niche conservatism as an emerging principle in ecology and conservation biology. *Ecol Lett* **13**: 1310-1324.
Yurkov A & Pozo MI (2017) Yeast Community Composition and Structure. *Yeasts in Natural Ecosystems: Ecology,*p.^pp. 73-100.
Yurkov AM (2018) Yeasts of the soil - obscure but precious. *Yeast* **35**: 369-378.
Zhang J, Saez-Sandino T, Maestre FT, Feng Y, Yu Y, Berdugo M, Wang J, Coleine C, Garcia-Velazquez L, Singh BK & Delgado-Baquerizo M (2025) Global environmental dependences of soil biodiversity and functions are modified by water availability thresholds. *Sci Total Environ* **958**: 178033.
Zhou SY, Lie Z, Liu X*, et al.* (2023) Distinct patterns of soil bacterial and fungal community assemblages in subtropical forest ecosystems under warming. *Glob Chang Biol* **29**: 1501-1513.

Supplementary Information

Supplementary Figures

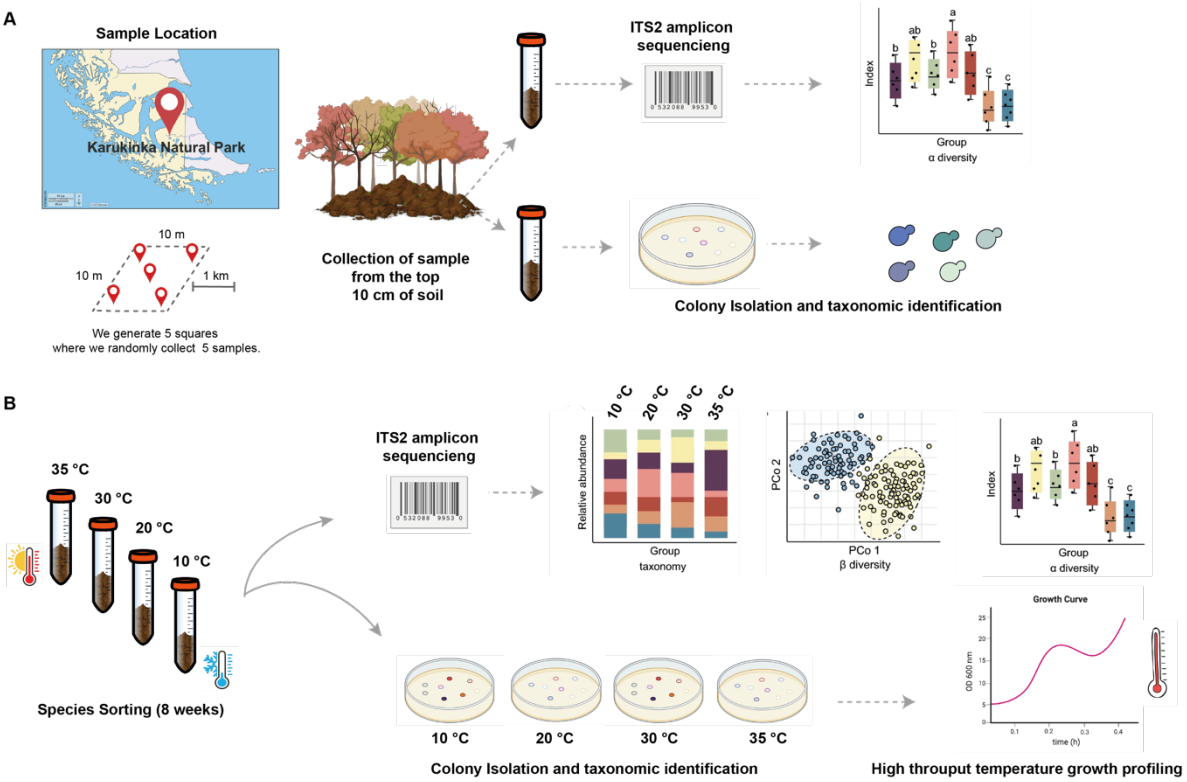

Figure S1. Experimental design used to evaluate the impact of temperature on culturable yeast communities. (A) Soil samples were collected from the top 10 cm of soil at Karukinka Natural Park (Tierra del Fuego, Chile) using five 10 × 10 m plots, each with five randomly selected sampling points. (B) Samples were incubated at 10, 20, 30, and 35 °C for eight weeks to assess species sorting across the thermal gradient. Yeasts were then isolated for taxonomic identification and subjected to ITS2 amplicon sequencing and temperature growth profiling.

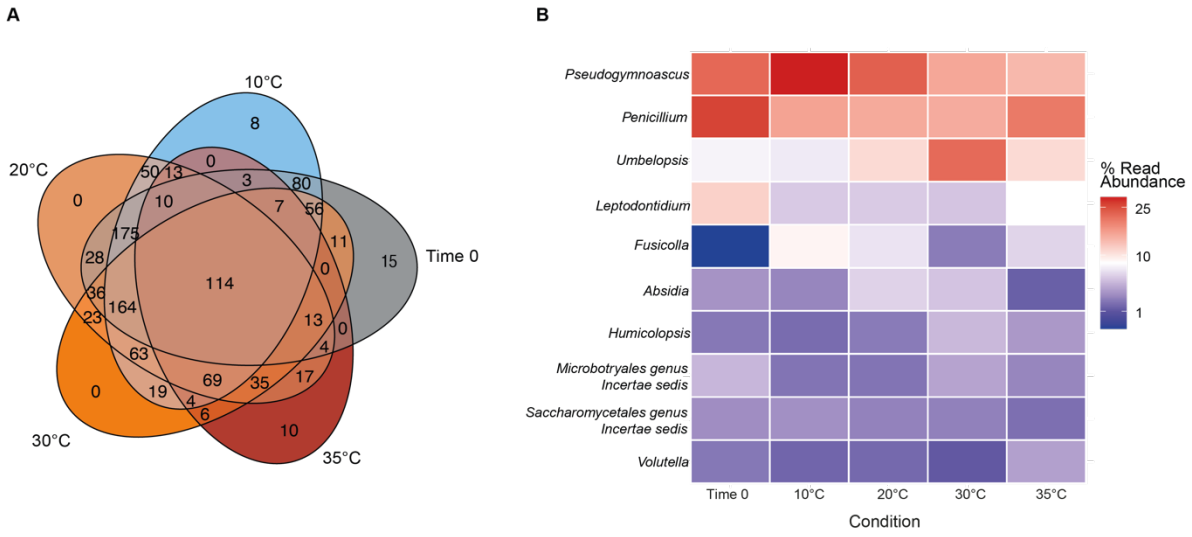

Figure S2. Overlap and relative abundance of dominant fungal genera across the temperature gradient. (A) Venn diagram showing the number of shared and unique fungal ASVs detected at each incubation temperature (Time 0, 10 °C, 20 °C, 30 °C, and 35 °C). (B) Heatmap representing the relative read abundance (% of total reads) of the top ten most abundant fungal genera across temperature treatments. Warmer colors indicate higher relative abundance.

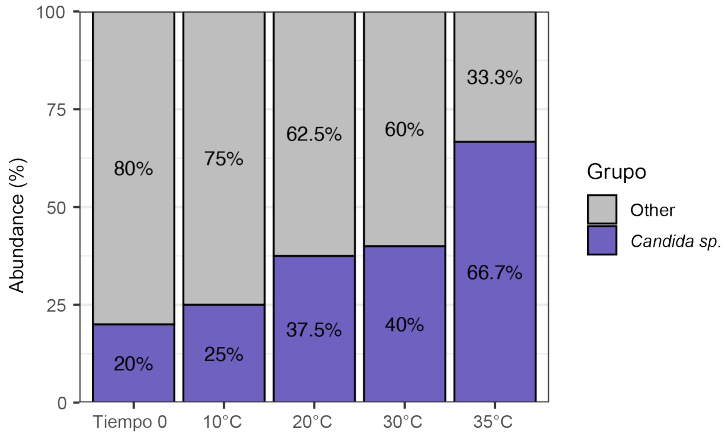

Figure S3. Relative abundance of *Candida* spp. across the thermal gradient. Stacked bar plots showing the proportion of *Candida* isolates (purple) and other yeasts (gray) recovered from Sub-Antarctic soil communities incubated at different temperatures (10 °C to 35 °C). Each bar represents the relative abundance within culturable communities at each temperature

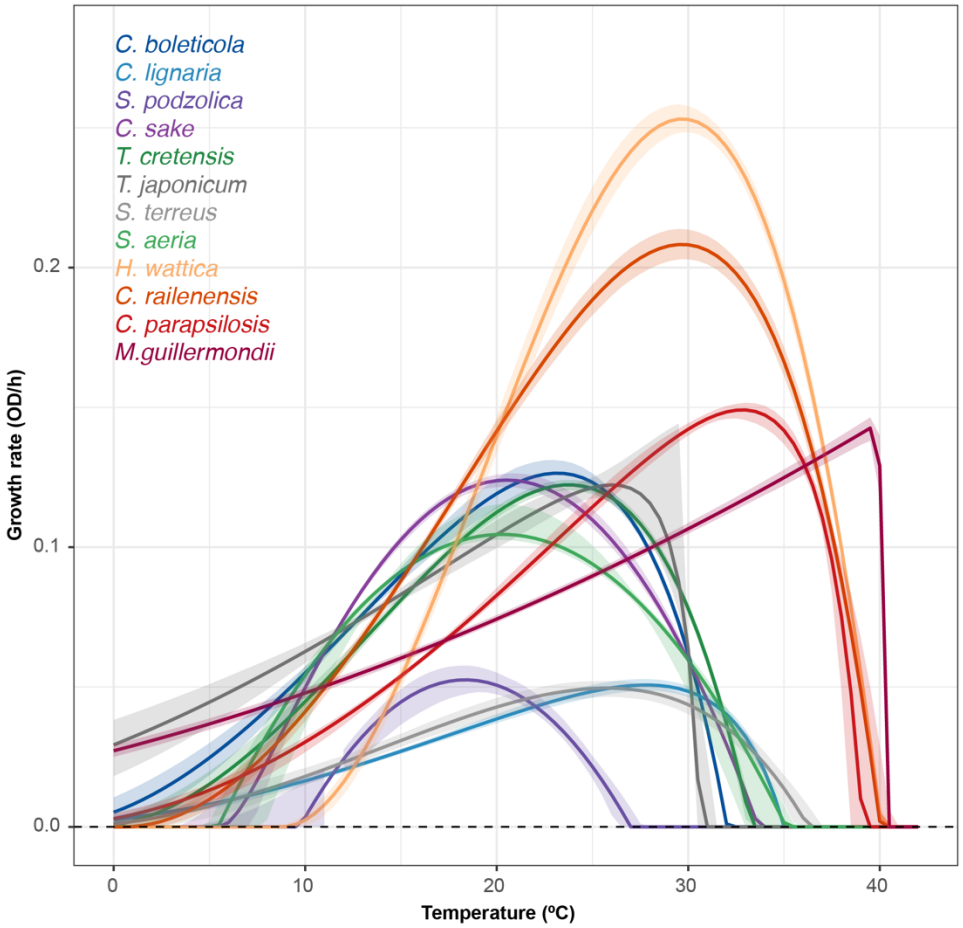

Figure S4. *Thermal performance curves (TPCs) of yeast species isolated from sub-Antarctic soils. TPCs were constructed using the CTMI fitting maximum growth rate values as a function of temperature for each species, using four independent replicates.*

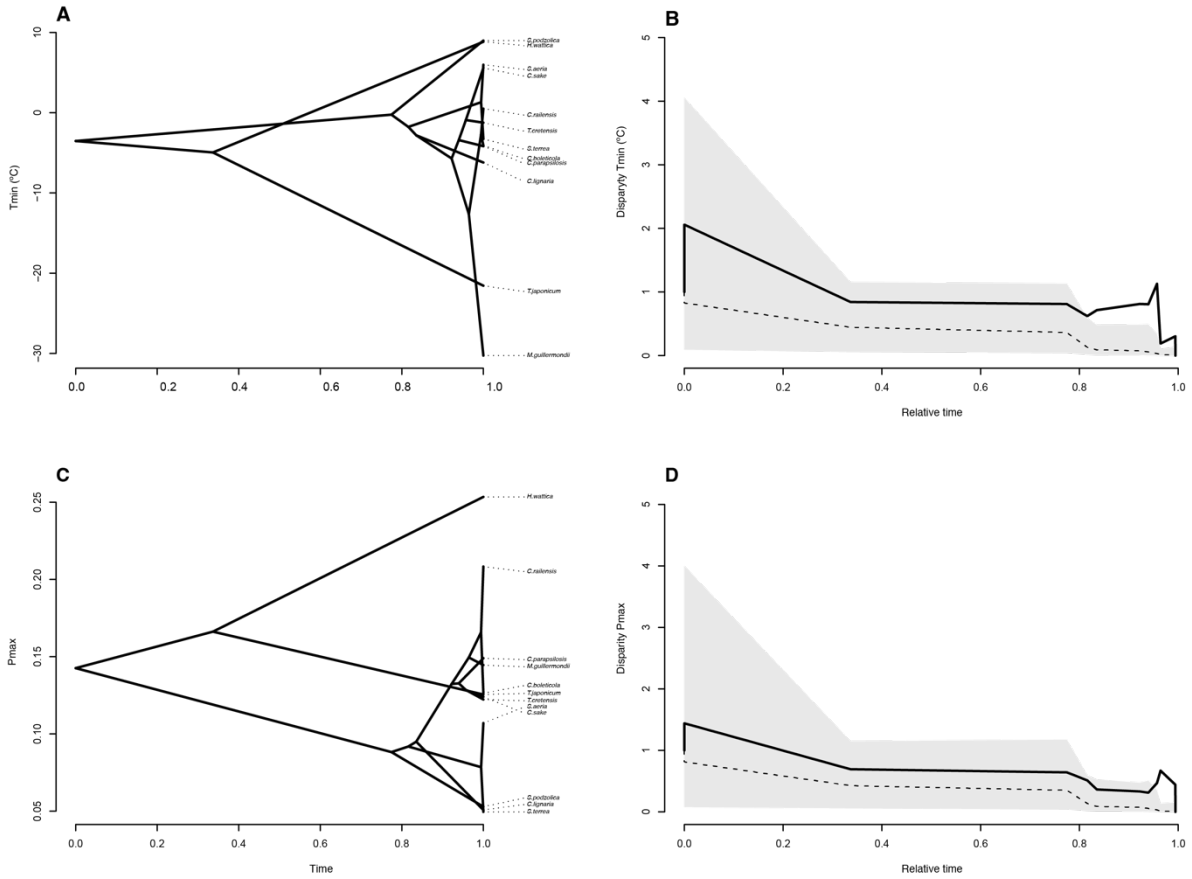

Figure S5. Phylogenetic trait evolution and disparity-through-time. Phenogram projecting the phylogenetic history of the studied taxa in relation to (A) T_{min} (Minimum temperature, °C), (C) P_{max}. The disparity-through-time plots for (B) T_{min} and (D) P_{max}. A simulation of the expectation of trait values assuming random walking evolution (dashed line), compared with what is observed (continuous line) in the trait of interest (percentage change in thermogenic capacity after cold acclimation). The gray area represents the 95% CI after 1000 simulations.

Supplementary Tables

Supplementary Table 1. Total number of raw reads
Supplementary Table 2. All ASV abundance table, taxonomy, and sample metadata
Supplementary Table 3. Filtered ASV abundance table, taxonomy, and sample metadata.
Supplementary Table 4. Core ASV abundance table.
Supplementary Table 5. Thermal sorting assay.
Supplementary Table 6. Thermal performance profiles of yeast species isolated from sub-Antarctic soils.
Supplementary Table 7. Phylogenetic models of traits.
Supplementary Table 8. Phylogenetic models using thermal performance curve variables.